# Modelling impacts of pollution in river systems: a new dispersion model and a case study of mine discharges in the Abrud, Aries and Mures River System in Transylvania, Romania

S. C. Chapra and P. G. Whitehead

## ABSTRACT

A new model of dispersion has been developed to simulate the impact of pollutant discharges on river systems. The model accounts for the main dispersion processes operating in rivers as well as the dilution from incoming tributaries and first-order kinetic decay processes. The model is dynamic and simulates the hourly behaviour of river flow and pollutants along river systems. The model has been applied to the Aries and Mures River System in Romania and has been used to assess the impacts of potential dam releases from the Roşia Montană Mine in Transylvania, Romania. The question of mine water release is investigated under a range of scenarios. The impacts on pollution levels downstream at key sites and at the border with Hungary are investigated.

**Key words** | cyanide, dispersion, mines, modelling, Mures River, Romania

**S. C. Chapra**
Department of Civil and Environmental Engineering,
Tufts University,
Medford 02155, MA,
USA

**P. G. Whitehead** (corresponding author)
Oxford University Centre for Water Research,
School of Geography and the Environment,
South Parks Road,
Oxford OX1 3YQ,
UK
E-mail: *paul.whitehead@ouce.ox.ac.uk*

## INTRODUCTION

Pollution downstream of abandoned mines is a major issue for many European countries and with legislation, such as the Water Framework Directive (WFD), there is an increasing need to clean up rivers sytems, restore the ecology and improve the status of river systems. It is well known that mine effluents and acid rock drainage (ARD) can have significant impacts on river systems (Nordstrom *et al.* 2000). ARD is the term used to describe the release of highly acidic waters that often arise from abandoned mines: the acid waters normally contain very high levels of toxic metals. Many active and passive treatment systems have been designed to control ARD (Johnson & Hallberg 2005) and extensive studies have been conducted to evaluate both active and passive wetland systems of remediation (Neal *et al.* 2005; Whitehead & Prior 2005; Whitehead *et al.* 2005*a*,*b*). The issue of mine closure and ARD is particularly acute in many European countries where historical mining has been undertaken with poor pollution control and where the high costs of treatment ensure that restoration remains an ongoing problem. Also, a key issue is the subsequent redevelopment of the old mines once Eastern European countries have recovered economically. The legacy of the past has to be cleaned up (Whitehead *et al.* 2009) and new problems may arise in order to meet modern safety and environment standards required by European Legislation.

In this paper we are concerned with an old mine at Roşia Montană, in the Transylvania Region of Romania (Figure 1). A new dispersion model has been developed to model pollution impacts on river systems. The model has been applied to the Roşia Montană Catchments and the Aries and Mures River System downstream. The model has been used to investigate a range of impact strategies and is concerned, in particular, with the release of cyanide from the tailings dam and this issue is addressed in this paper. The impacts of the mine discharges on metal concentrations in the rivers and potential future restoration strategies are addressed by Whitehead *et al.* (2009).

doi: 10.2166/nh.2009.075


**Figure 1** | Romania and the location of Roşia Montană.

## THE ROŞIA MONTANĂ MINE AND THE DOWNSTREAM RIVER SYSTEM

The Roşia Montană mining site lies in the northwest of Romania, as shown in Figure 1, and is located in the Apuseni Mountains, which are part of the Carpathian Mountains in Transylvania. The Roşia Montană catchments drain into the Abrud and Aries River system which subsequently flows into the Mures River, as shown in Figure 2. Downstream of the Romanian-Hungarian Border, the Mures River joins the Tisza River before joining the River Danube.

The Roşia Montană area has a long history of mining, including periods of Roman, Dacian and Austro-Hungarian works. There are up to 140 km of historical mining galleries, in which acid rock drainage (ARD) has been, and still is, actively generated. As a result, surface and groundwater are contaminated by heavy metals and this has a major impact on downstream rivers. There is therefore a need to reduce the ARD and, through the use of EU-compliant mining methods, to restore the quality of the waters draining into the Abrud, Aries and Mures Rivers. As part of this restoration process, there is planning for large-scale open-pit mining of gold and silver at Roşia Montană as well as the collection of the spoil rock into a self-contained system with leakage control (Aston 2004).

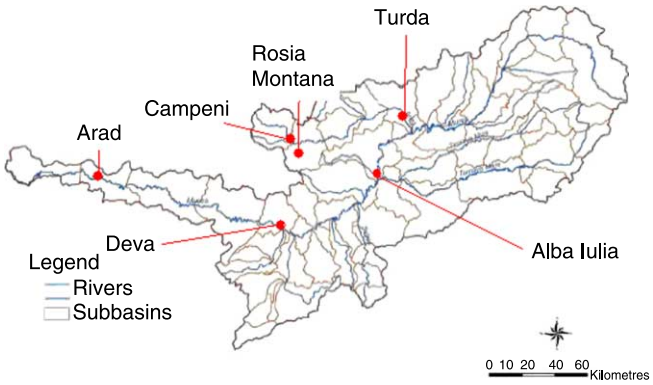


**Figure 2** | The Mures River basin, key locations and sub-catchments.

These control sites will be re-vegetated and mine drainage (including historical ARD) will be collected and treated before discharge. Metal release is therefore a key issue for such mine systems; the mine impacts and proposed clean-up operation has been investigated by Whitehead *et al.* (2009). Another important water quality parameter that requires investigation is that of cyanide, for which the Hungarian standard is $0.1\,mg\,l^{-1}$ CN WAD (weak acid dissociable) for high-quality rivers. With respect to cyanide, a key standard is the new Best Available Technology standards for cyanide for mine storage waters. The new EU Directive on Waste Management stipulates CN must be below the $10\,mg\,l^{-1}$ level in mine storage dams, which is well below the previous EU standard of $50\,mg\,l^{-1}$.

A key question concerning the Roşia Montană development is the impact of the restoration strategies and potential dam failure scenarios on the downstream water quality. In this current study, this question is addressed using a new process-based and dynamic dispersion model. The model is tested for the upstream catchments and then applied to the full river system, down as far as the Hungarian Border at Nadlac on the Mures River. A suite of scenarios are investigated to evaluate the potential impacts of cyanide releases from the tailing dam in the event of an accidental dam discharge.

## DISPERSION MODELLING OF POLLUTANT SPILLS

A new model has been developed to numerically simulate the transport and fate of a river contaminant spill. The model is based on the classical dispersion Equation (Fischer 1968) but also incorporates the dilution effects of tributaries joining the main river as well as any chemical decay processes occurring in the river system. The model assumes that lateral and vertical gradients are minimal and that the contaminant

can decay with first-order kinetics. The general nature of this model is particularly useful as it would be possible to apply the model to any pollutant that has first-order chemical decay or kinetics and almost any river system which is subject to lateral inflows of water that give rise to the dilution effect. The model could therefore be used for radioactive discharges, pesticides, *E. coli* and any pollutant that can be approximately represented as a simple chemical decay.

In the case of cyanide the chemistry is considered complex when in a pond situation, as indicated by Mudder *et al.* (2001). However Simovic *et al.* (1984) and Botz & Mudder (2001) have shown that the dominant volatilization and degradation processes can be represented by first-order kinetics. In river systems, where there is significant turbulence and mixing, these two key processes also control cyanide losses and can be represented by first-order kinetics dependent on temperature, concentration and river residence time. This kinetic approach to modelling metals and pollutants has been used successfully in the Wheal Jane Mine study by Whitehead *et al.* (2005*b*), and this is the approach adopted for the modelling of the metals and cyanide in the current study.

## Segmentation

In order to derive a numerical solution the river is divided into a series of reaches, as shown in Figure 3. These reaches represent river segments that have constant hydrogeometric characteristics but the reaches can be of different lengths. The reaches themselves are further divided into a series of equal length computational elements. The elements represent the fundamental units for which water and mass balances are written and solved.

In summary, the nomenclature used to describe the way in which the spill model organizes river topology is as follows.

- Reach: a length of river with constant hydraulic characteristics.
- Element: the model's fundamental computational unit which consists of an equal length subdivision of a reach.

## Initial flow balance

A steady-state flow balance is implemented for each model element. For the first element in a reach, the budget is written as (see Figure 4):

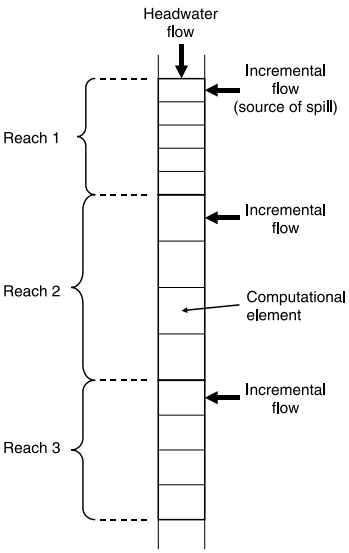


**Figure 3** | Spill model segmentation scheme showing reaches divided into equal-sized computational elements (the system's external flows are also depicted).

$$Q_i = Q_{i-1} + Q_{\text{in},i} \tag{1}$$

where $Q_i$ = outflow from element $i$ into the downstream element $i+1$ ($m^3 s^{-1}$), $Q_{i-1}$ = inflow from the upstream element $i-1$ ($m^3 s^{-1}$), and $Q_{\text{in},i}$ is the incremental inflow into the element from point and non-point sources along the length of the reach ($m^3 s^{-1}$). Thus, the downstream outflow of the first element is simply the sum of the inflow from upstream and the incremental flow. For the other elements of the reach $Q_{\text{in},i} = 0$ and, therefore, outflow equals inflow i.e. $Q_i = Q_{i-1}$.

## Depth, velocity and other hydraulic parameters

Once the outflow for each element is computed, the depth $H_i$ (m) and velocity $U_i$ ($m s^{-1}$), are calculated in one of two ways: rating curves and the Manning equation.

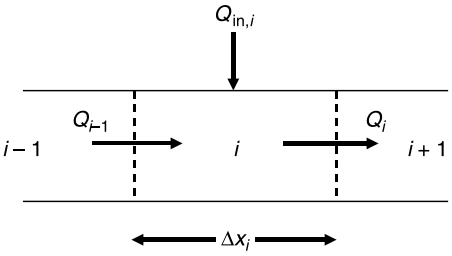


**Figure 4** | Flow balance for the first element in a reach.

### Rating curves

Rating curves in the form of power equations are used to relate mean velocity and depth to flow for each element:

$$U_i = aQ_i^b \tag{2}$$

$$H_i = \alpha Q_i^\beta \tag{3}$$

where $U_i$ = the mean velocity across the downstream interface of element $i$ ($\mathrm{m\,s^{-1}}$), $H_i$ = the average depth of element $i$ (m) and $a$, $b$, $\alpha$ and $\beta$ are empirical coefficients that are determined from velocity–discharge and stage–discharge rating curves, respectively. Note that the sum of $b$ and $\beta$ must be less than or equal to 1. If this is not the case, the width will decrease with increasing flow. If their sum equals 1, the channel is rectangular.

After the velocity and depth of an element are computed with Equations (2) and (3), they can be used to compute other required hydrogeometric characteristics. For example, the velocity can be substituted into the continuity Equation ($Q_i = U_i\ A_{c,i}$) to determine the element's cross-sectional area ($\mathrm{m^2}$):

$$A_{c,i} = \frac{Q_i}{U_i}. \tag{4}$$

The area can be directly related to flow by substituting Equation (2) into Equation (4) to give

$$A_{c,i} = \frac{Q_i}{aQ_i^b} = \frac{1}{a}Q_i^{1-b}. \tag{5}$$

The element's mean width $B$ (m), wetted perimeter $P$ (m) and volume $V$ ($\mathrm{m^3}$) follow

$$B_i = \frac{A_{c,i}}{H_i} \tag{6}$$

$$P_i = B_i + 2H_i \tag{7}$$

$$V_i = B_i H_i \Delta x_i \tag{8}$$

where $\Delta x_i$ = the element length (m).

Besides computing the hydrogeometric characteristics as a function of flow, the rating curves can also be employed to perform the inverse calculation. That is, given volume, they can also be used to compute flow, depth, velocity, area, width and wetted perimeter. Because $\Delta x$ is known, we first determine the cross-sectional area as:

$$A_{c,i} = \frac{V_i}{\Delta x_i} \tag{9}$$

Flow can then be evaluated by solving Equation (5) for

$$Q_i = a^{1/(1-b)}A_c^{1/(1-b)}. \tag{10}$$

Once flow is known, Equations (2), (3), (6) and (7) can be then employed to compute $U_i$, $H_i$, $B_i$, and $P_i$.

### Manning equation

Each element in a particular reach is idealized as a trapezoidal channel (Figure 5). For such channels, the Manning Equation can be used to express the relationship between flow and depth as

$$Q_i = \frac{S_{0,i}^{1/2}}{n_i}\frac{A_{c,i}^{5/3}}{P_i^{2/3}} \tag{11}$$

where $S_{0,i}$ = bottom slope ($\mathrm{m\,m^{-1}}$), $n_i$ = the Manning roughness coefficient, $A_{c,i}$ = the cross-sectional area ($\mathrm{m^2}$) and $P_i$ = the wetted perimeter (m).

The cross-sectional area and wetted perimeter are computed as

$$A_{c,i} = (B_{0,i} + s_i H_i)H_i \tag{12}$$

$$P_i = B_{0,i} + 2H_i\sqrt{s_i^2 + 1} \tag{13}$$

where $B_{0,i}$ = bottom width (m) and $s_i$ = the side slope as shown in Figure 5 ($\mathrm{m\,m^{-1}}$). Substituting Equations (12) and (13) into (11) gives

$$Q_i = \frac{1}{n_i}\frac{[(B_{0,i} + s_i H_i)H_i]^{5/3}}{\left[B_{0,i} + 2H_i\sqrt{s_i^2 + 1}\right]^{2/3}}S_{0,i}^{1/2}. \tag{14}$$

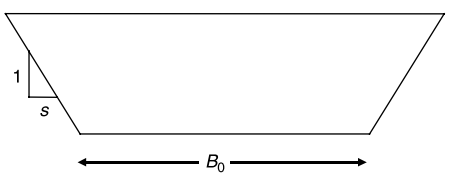


**Figure 5** | A cross-section of a trapezoidal channel showing the parameters needed to uniquely define the geometry: $B_0$ = bottom width, $s$ = side slope.

Given values for $Q$, $B_0$, $S_0$, $n$ and $s$, Equation (14) is a nonlinear Equation with one unknown $H$ which can be reformulated as

$$f(H_i) = \frac{1}{n_i}\frac{[(B_{0,i} + s_i H_i)H_i]^{5/3}}{\left[B_{0,i} + 2H_i\sqrt{s_i^2 + 1}\right]^{2/3}} S_{0,i}^{1/2} - Q_i. \quad (15)$$

The root (i.e. the value of depth that makes this Equation zero) is the reach depth. It can be shown that the root can be determined efficiently by successive substitution (Chapra & Canale 2006) using the iterative formula:

$$H_{i,k} = \frac{(Q_i n_i)^{3/5}\left(B_{0,i} + 2H_{i,k-1}\sqrt{s_i^2 + 1}\right)^{2/5}}{S_{0,i}^{3/10}[B_{0,i} + s_i H_{i,k-1}]} \quad (16)$$

where $k = 1, 2, \ldots, n$, where $n$ = the number of iterations. If an initial guess of $H_{i,0} = 0$ is employed, this approach is rapidly convergent for all natural channels (Chapra & Canale 2006). The method is terminated when the estimated error falls below a specified value of 0.001%. The estimated error is calculated as

$$\varepsilon_{a,i} = \left|\frac{H_{i,k+1} - H_{i,k}}{H_{i,k+1}}\right| \times 100\% \quad (17)$$

Once the depth is known, the cross-sectional area and wetted perimeter are computed with Equations (12) and (13), and the velocity can be determined from the continuity equation:

$$U_i = \frac{Q_i}{A_{c,i}} \quad (18)$$

The average element width, $B_i$ (m) is then computed as

$$B_i = \frac{A_{c,i}}{H_i}, \quad (19)$$

the top width, $B_{1,i}$ (m) as

$$B_{1,i} = B_{0,i} + 2s_i H_i \quad (20)$$

and the element volume as

$$V_i = B_i H_i \Delta x_i. \quad (21)$$

As was the case with the rating curves, the Manning approach can also be employed to perform the inverse calculation. If the volume is given, the cross-sectional area can be generated with Equation (9). The depth is determined by reformulating Equation (12) as a quadratic, i.e.

$$s_i H_i^2 + B_{0,i} H_i - A_{c,i} = 0. \quad (22)$$

The positive root of this equation yields the depth (note that this version of the quadratic formula prevents division by zero for rectangular channels i.e. with $s_i = 0$):

$$H_i = \frac{2A_{c,i}}{B_{0,i} + \sqrt{B_{0,i}^2 + 4s_i A_{c,i}}}. \quad (23)$$

The average width and flow are computed with Equations (19) and (14), respectively, and the velocity then follows from Equation (18).

## Dynamic water balance

After the initial volumes are determined, the software generates a numerical solution of the one-dimensional continuity equation:

$$\frac{\partial A_c}{\partial t} = -\frac{\partial Q}{\partial x} \quad (24)$$

Equation (24) can be expressed in numerical form by writing a water balance around each element to give

$$\frac{dV_i}{dt} = Q_{i-1} + Q_{i,\text{in}} - Q_i \quad (25)$$

where $Q_i$ is the outflow which is computed as described previously. Equation (25) is then integrated numerically to obtain the element volumes as a function of time.

## Dispersion

Dispersion can either be user-prescribed or computed. In the latter case, based on Rutherford's (1994) assessment, three empirically-derived equations are available to compute the longitudinal dispersion for the downstream boundary between two elements.

According to Fischer *et al.* (1979),

$$E_{p,i} = 0.011 \frac{U_i^2 B_i^2}{H_i U_i^*} \tag{26}$$

where $E_{p,i}$ = the longitudinal dispersion between elements $i$ and $i+1$ ($m^2 s^{-1}$) and $U_i$ = mean velocity of element $i$ ($m s^{-1}$), $B_i$ = mean width (m), $H_i$ = depth (m) and $U_i^*$ = shear velocity ($m s^{-1}$), which is related to more fundamental characteristics by

$$U_i^* = \sqrt{g H_i S_{0,i}} \tag{27}$$

where $g$ = acceleration due to gravity ($= 9.81 m s^{-2}$) and $S_{0,i}$ = bottom slope ($m m^{-1}$).

According to Liu (1977),

$$E_{p,i} = 0.18 \left(\frac{U_i^*}{U_i}\right)^{1.5} \frac{Q_i^2}{U_i^* R_h^3} \tag{28}$$

where $R_h$ = the hydraulic radius (m), equal to the ratio of the cross-sectional area to the wetted perimeter.

According to McQuivey & Keefer (1974),

$$E_{p,i} = 0.058 \frac{Q_i}{S_i B_i}. \tag{29}$$

This formulation is limited to systems with Froude numbers ($F = U/\sqrt{gH}$) less than 0.5. If this constraint is exceeded, the software automatically displays an error message and terminates.

## Mass balance

The software generates a numerical solution of the one-dimensional advection-dispersion-reaction equation:

$$\frac{\partial c}{\partial t} = -\frac{\partial Uc}{\partial x} + \frac{\partial}{\partial x}\left(E \frac{\partial c}{\partial x}\right) - kc \tag{30}$$

where $c$ = concentration ($mg l^{-1}$), $t$ = time (s), $U$ = velocity ($m s^{-1}$), $x$ = distance (m), $E$ = dispersion ($m^2 s^{-1}$) and $k$ = first-order decay rate ($d^{-1}$).

Equation (30) can be expressed in numerical form by writing a mass balance around each element, as shown in Figure 6. In order to account for the non-uniformity, as well as to conserve mass, the fluxes between elements are

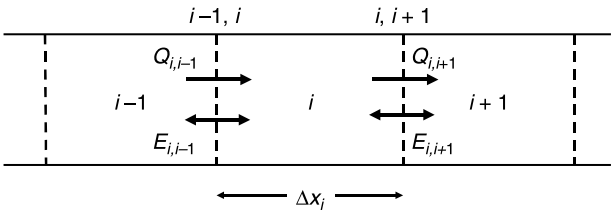


**Figure 6** | One-dimensional channel divided into a series of elements.

specified at their upstream and downstream faces to give:

$$\frac{\partial M_i}{\partial t} = \left(UA_c c - EA_c \frac{\partial c}{\partial x}\right)_{i-1,i} - \left(UA_c c - EA_c \frac{\partial c}{\partial x}\right)_{i,i+1} - kV_i c_i \tag{31}$$

where $M_i$ = the mass of pollutant in element $i$ (g) = $V_i c_i$.

Assuming that the concentrations at each interface are equal to the upstream element (i.e. a backward or 'upstream' difference), and using centred differences for the gradients, yields:

$$\frac{dM_i}{dt} = W(t) + Q_{i-1,i} c_{i-1} - Q_{i,i+1} c_i + E_{i-1,i} A_{c,i-1,i} \frac{c_{i-1} - c_i}{\Delta x_{i-1,i}} + E_{i,i+1} A_{c,i,i+1} \frac{c_{i+1} - c_i}{\Delta x_{i,i+1}} - kV_i c_i \tag{32}$$

where $W(t)$ = mass loading rate ($g s^{-;1}$), $Q_{j,k}$ = the flow from element $j$ into element $k$ ($m^3 s^{-1}$), $E_{j,k}$ = the dispersion between elements $j$ and $k$ ($m^2 s^{-1}$) and $\Delta x_{j,k}$ = the length between the mid-points of elements $j$ and $k$ (m):

$$\Delta x_{j,k} = \frac{\Delta x_j + \Delta x_k}{2} \tag{33}$$

where $\Delta x_i$ = the length of element $i$ (m). This equation can then be written for all the elements and integrated numerically to obtain the solution.

## Solution method

Equations (25) and (32) are solved numerically with Euler's method as follows:

1. Determine and save the initial values for all elements.
2. Compute derivatives with Equations (25) and (33).
3. Compute new volumes and masses with Euler's method:

$$V_i(t + \Delta t) = V_i(t) + \frac{dV_i(t)}{dt} \Delta t$$

$$M_i(t + \Delta t) = M_i(t) + \frac{dM_i(t)}{dt}\Delta t$$

4. Compute new outflows for each element as a function of their new volumes.
5. Compute other hydraulic parameters.
6. Compute new concentrations: $c_i = M_i/V_i$.
7. Increment time: $t = t + \Delta t$.
8. Save new values. If $t \geq$ final time, exit to Step 10.
9. Loop back to Step 2.
10. Display results.

In the absence of numerical dispersion, the foregoing hydraulic solution is similar to the kinematic wave. However, because of the use of first-order forward time differencing and backward space differencing, it does exhibit numerical dispersion and hence is more akin to a diffusive wave solution. Techniques such as the Muskingum-Cunge method attempt to mitigate such effects; the solution time-step is selected in order that the numerical dispersion approximates the actual diffusion exhibited by waves subject to gravity effects.

In a similar fashion, the mass solution also generates additional numerical dispersion. As with the hydraulics, a time-step can be chosen in an attempt to match the numerical dispersion to the actual dispersion.

Unfortunately, different time-steps are needed for the hydraulic and mass solutions. Further, because the system being studied has a wide range of flows and velocities, the optimal time-step will vary greatly. The following scheme attempts to minimize the impact of both effects while using a single time-step.

For the mass solution, the total dispersion generated consists of the model dispersion, $E_i$, along with some additional numerical dispersion, $E_{n,i}$. Since we would like the solution to have the correct physical dispersion (i.e. either user-specified or computed with Equations (26)–(29)) $E_{p,i}$, we therefore desire that

$$E_{p,i} = E_i + E_{n,i}. \tag{34}$$

A Taylor series expansion (Chapra 1997) can be used to relate the numerical dispersion to the space and time-steps as

$$E_{n,i} = 0.5U_i\Delta x_i - 0.5U_i^2\Delta t. \tag{35}$$

Substituting Equation (35) into (34) and rearranging yields

$$E_i = E_{p,i} - 0.5U_i\Delta x_i + 0.5U_i^2\Delta t. \tag{36}$$

Therefore, to achieve accuracy, the dispersion used in the model $E_i$ is automatically set equal to the desired dispersion: $E_{p,i}$ minus the numerical dispersion $E_{n,i}$.

There are two stability constraints. First, a spatial positivity constraint can be formulated as

$$\Delta x_i < \frac{2E_i}{U_i}. \tag{37}$$

This constraint guarantees positive solutions.

In addition, the time-step is constrained according to

$$\Delta t < \frac{\Delta x_i^2}{U_i\Delta x_i + 2E_i + k\Delta x_i^2} \tag{38}$$

where the right-hand side is the element's residence time (s). This is the analogue of the Courant condition for Equation (32). These criteria can be used to develop a solution procedure that maximizes accuracy and guarantees stability as described next.

First, the user specifies the maximum desired size of the element length for each reach. Then, Equation (37) is used to determine the maximum permissible size based on the velocity and the dispersion, i.e. using $E_i = E_{p,i}$. If the desired size is greater than the permissible size, the element length is set to the permissible size. Otherwise, the element length is set to the maximum desired size. The resulting element length is then divided into the reach length and the result rounded up in order to determine the number of elements for each reach.

Second, Equation (38) is used to determine a maximum allowable time-step for each reach. The minimum of these time-steps is then taken as the computational time-step for the entire system.

Finally, this time-step along with the element size is substituted into Equation (35) to compute the numerical dispersion. If it is less than the physical dispersion, Equation

(36) is used to compute the dispersion coefficient that should be input to the model.

## APPLICATION OF THE DISPERSION MODEL TO THE ARIES-MURES RIVER SYSTEM

The dispersion model has been applied to simulate the river system downstream of the mine and a range of worst-case scenarios. There are two extremes of weather that can create worst case conditions: (1) an incident associated with high rainfall or snowmelt event in the mountains area of Roşia Montană during a low-flow condition downstream; or (2) a high rainfall or snow event when the rivers are in flood conditions. In the first low-flow case, dilution is low but the travel time is relatively high due to the low water velocity, whereas in the second case the high flows generate significant dilution but velocities are fast with low travel times along the river.

There are also two types of major incident. Firstly, there is a catastrophic event such as occurred at Baia Mare in 2000 when very high precipitation significantly raised the water level in a mine storage dam and an overflow release occurred (UNEP 2000). The second type is associated with a significant failure of the dam wall with a sudden release of polluted water. Both of these types of incident are considered here.

### River model set-up

Much of the detailed characteristics of the river system have already been described by Whitehead *et al.* (2009). Essentially, the dispersion model has been set up in the same manner as the INCA model (Whitehead *et al.* 2009) from the location of the proposed dam in the Corna catchment above Abrud down to the Aries River and then into the Mures River down to the border at Nadlac. Hydrogeometric information (e.g. elevations, slopes, locations of reaches, etc.) is provided in the INCA model application to the river system (Whitehead *et al.* 2009). However, Table 1 gives additional information on velocity and depth conditions in the rivers under high, medium and low-flow conditions. Table 2 summarizes the low-flow (95th percentile) and high-flow (5th percentile) conditions that have been used in the model runs.

**Table 1** | Depth and velocity information at a range of locations and under a range of flow conditions

| River | Aries | Aries | Mures | Mures | Mures |
|---|---|---|---|---|---|
| Location | Campeni | Baia de Aries | Ludus | Alba Iulia | Branisca |
| Depth (m) | | | | | |
| High flows | 2.72 | 3.53 | 5.36 | 3.00 | 4.70 |
| Medium flows | 0.50 | 0.76 | 1.13 | 1.25 | 1.55 |
| Low flows | 0.23 | 0.38 | 0.37 | 0.60 | 0.43 |
| Velocity ($m\,s^{-1}$) | | | | | |
| High flows | 2.69 | 2.75 | 1.20 | 1.65 | 1.86 |
| Medium flows | 1.72 | 1.58 | 0.98 | 1.20 | 1.25 |
| Low flows | 0.37 | 0.21 | 0.18 | 0.37 | 0.48 |

### Velocity calculation

A key issue of concern is whether to use the observed depth and velocity information provided in Table 1 to estimate travel times within the model or to use a formula such as the Manning equation. The problem with the observed data is that it is only available at a limited number of sites along the river. The river systems of the Abrud, the Aries and the Mures are complex natural rivers with highly variable geometry and highly variable flow conditions. The collection of field data to provide the necessary level of detail over a range of flow conditions and at all sites of interest over 550 km of river is a major task. However, we have used the available depth and velocity data to create rating equations and used these in

**Table 2** | Low–and high-flow conditions for the Abrud, Aries and Mures Rivers

| River | Reach location | Q 95th percentile ($m^3\,s^{-1}$) | Q 5th percentile ($m^3\,s^{-1}$) |
|---|---|---|---|
| Abrud | Campeni | 0.06 | 164 |
| Aries | Campeni | 0.96 | 320 |
| Aries | Baia de Aries | 1.44 | 455 |
| Aries | Buru | 1.64 | 610 |
| Aries | Turda | 1.66 | 640 |
| Mures | Ludus | 4.35 | 1,020 |
| Mures | Alba Iulia | 9.5 | 1,404 |
| Mures | Gelmar | 15.8 | 1,436 |
| Mures | Branisca | 16.4 | 1,458 |
| Mures | Savarsin | 17.1 | 1,431 |
| Mures | Nadlac | 20.5 | 1,404 |

**Table 3** | A comparison of simulated CN concentration estimates using both rating equations and Manning's equations for high-flow conditions

| Location | Time (days) | Manning equation peak CN conc ($mg\,l^{-1}$) | Rating equation peak CN conc ($mg\,l^{-1}$) |
|---|---|---|---|
| Abrud | 0.11759 | 0.33725 | 0.33472 |
| Campeni | 1.00815 | 0.17961 | 0.17934 |
| Baia de Aries | 1.03241 | 0.12778 | 0.12771 |
| Turda | 1.15444 | 0.09160 | 0.09152 |
| Ocna Mures | 1.32426 | 0.05789 | 0.05786 |
| Albalulia | 1.82537 | 0.04225 | 0.04225 |
| Deva | 2.46593 | 0.04132 | 0.04132 |
| Savirsin | 3.39611 | 0.04070 | 0.04070 |
| Arad | 3.72407 | 0.04014 | 0.04014 |
| Nadlac | 4.00315 | 0.03961 | 0.03961 |

the model to simulate pollutant transport. In addition, we have built into the model the conventional Manning equation such that it can be applied at every location and under any flow condition. We have compared the concentrations simulated using the two different velocity estimation techniques.

Table 3 shows the simulated concentrations of CN WAD using the two approaches. The results are, in fact, very similar and it is considered that both approaches are acceptable for these river systems.

**Table 4** | The CN concentrations in the dam during a Baia Mare type event

| Assuming 1 in 10 year flood spillway flow of $2.3\,m^3\,s^{-1}$ | CN total concentration behind the dam ($mg\,l^{-1}$) |
|---|---|
| Summer–initial dam condition year 1 | 0.36 |
| Summer–final dam conditions year 17 | 1.09 |
| Winter–initial dam condition year 1 | 1.09 |
| Winter–final dam conditions year 17 | 3.27 |

**Table 5** | Simulated peak CN WAD concentrations assuming a Baia Mare type event under low-flow summer conditions assuming a final dam condition

| Reach | Travel time days | CN conc ($mg\,l^{-1}$) |
|---|---|---|
| Abrud | 0.501 | 0.888 |
| Campeni | 0.604 | 0.637 |
| Baia de Aries | 1.022 | 0.396 |
| Turda | 3.186 | 0.105 |
| Ocna Mures | 5.737 | 0.029 |
| Albalulia | 10.173 | 0.009 |
| Deva | 13.971 | 0.004 |
| Savirsin | 18.582 | 0.002 |
| Arad | 20.152 | 0.002 |
| Nadlac | 21.483 | 0.001 |

**Table 6** | Simulated peak CN WAD concentrations assuming a Baia Mare type event under low-flow winter conditions assuming a final dam condition

| Reach | Travel time (days) | CN conc ($mg\,l^{-1}$) |
|---|---|---|
| Abrud | 0.501 | 2.659 |
| Campeni | 0.606 | 1.952 |
| Baia de Aries | 1.037 | 1.272 |
| Turda | 3.332 | 0.422 |
| Ocna Mures | 5.947 | 0.150 |
| Albalulia | 10.472 | 0.077 |
| Deva | 14.329 | 0.053 |
| Savirsin | 18.999 | 0.041 |
| Arad | 20.588 | 0.036 |
| Nadlac | 21.933 | 0.033 |

## Dispersion coefficient calculation

Another issue when modelling river water quality is how to estimate the dispersion coefficients in river systems. A series of tracer experiments to estimate these for all three rivers over a total of 30 reaches under a full range of flow conditions is a major undertaking, requiring considerable

**Table 7** | Simulated peak CN WAD concentrations assuming a Baia Mare type event under high-flow (Q5) winter conditions assuming a final dam condition

| Reach | Travel time (days) | CN conc ($mg\,l^{-1}$) |
|---|---|---|
| Abrud | 0.108 | 0.045 |
| Campeni | 0.122 | 0.045 |
| Baia de Aries | 0.509 | 0.023 |
| Turda | 0.533 | 0.016 |
| Ocna Mures | 0.692 | 0.012 |
| Albalulia | 0.976 | 0.007 |
| Deva | 1.684 | 0.005 |
| Savirsin | 2.350 | 0.005 |
| Arad | 3.237 | 0.005 |
| Nadlac | 3.815 | 0.005 |

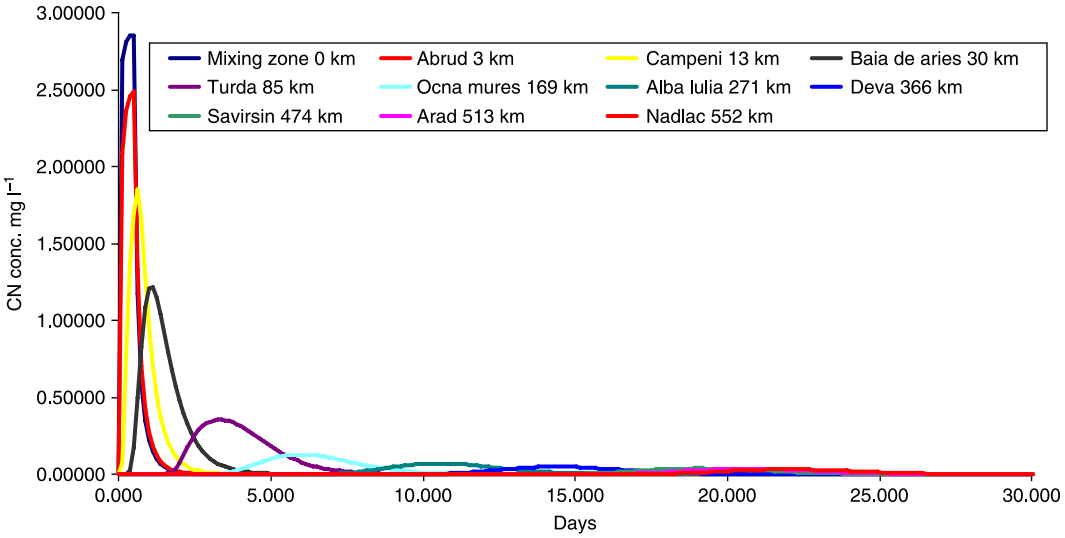


**Figure 7** | CN WAD simulation of a Baia Mare type rainfall/snow event for the Mures River System under low-flow winter conditions assuming a final TMF condition.

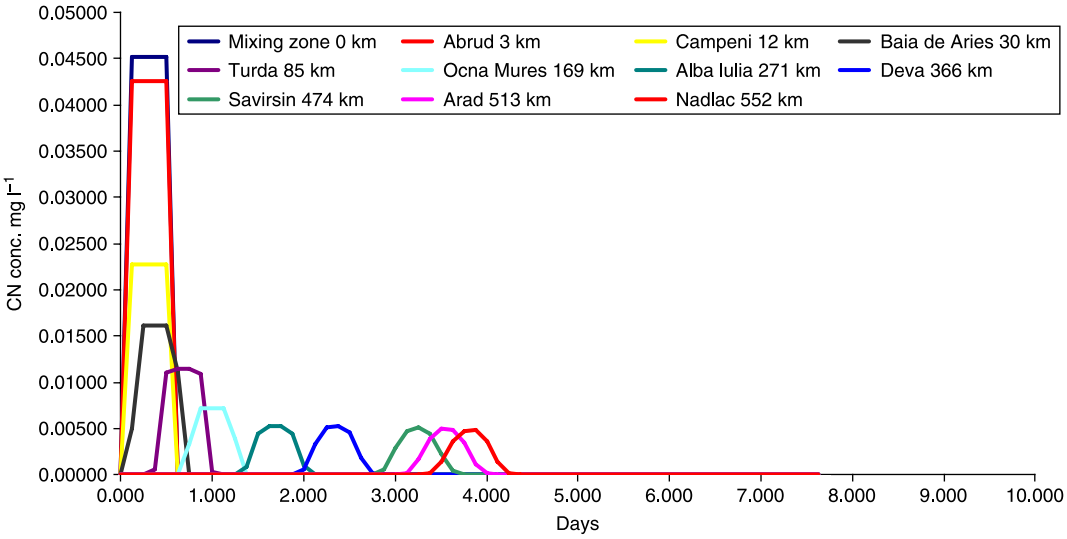


**Figure 8** | CN simulation of a Baia Mare type rainfall/snow event for the Mures River System under high-flow (Q5) winter conditions assuming a final dam condition.

**Table 8** | The set of scenarios with a combination of dam failures and river flow conditions

| Scenario | Pond CN WAD concentrations (mg $l^{-1}$) | Dam failure timing | Dam release water volume ($m^3$) | River discharge conditions |
|---|---|---|---|---|
| 3a | 4.8 | Year 1 | 1,078,000 | low |
| 3b | 4.8 | Year 1 | 1,078,000 | high |
| 3c | 4.4 | Year 17 | 3,811,200 | low |
| 3d | 4.4 | Year 17 | 3,811,200 | high |
| 3e | 5.0 | Year 17 | 5,880,800 | low |
| 3f | 5.0 | Year 17 | 5,880,800 | high |

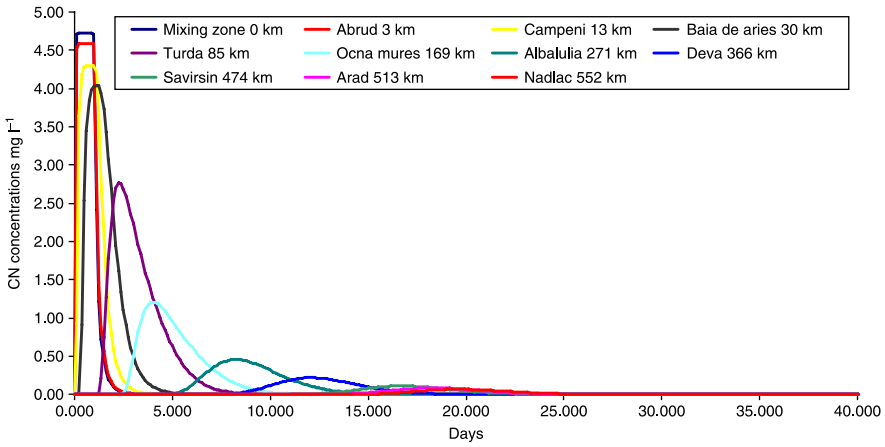


**Figure 9** | Simulation of scenario 3a under low-flow conditions assuming a decay of 0.1 days$^{-1}$.

time to complete. Probably many years would be required to cover the full range of flow conditions.

There are also significant practical difficulties. For example, the only tracers that could be used effectively to give adequate dilution are either radioactive tracers or fluorescent tracers such as Rhodamine WT. These can be measured down to microgram/litre concentrations. However, in many European countries (e.g. UK) the Rhodamine tracer has been banned because of water colour problems (the tracer colours the water bright red) and there are also potential health hazard problems associated with Rhodamine.

Similarly, there are significant health problems with radioactive tracers. Another tracer that is often used is Potassium Iodide (Whitehead *et al.* 1986), which can also be measured to low concentrations. However, this tracer is often adsorbed onto fine sediments. Hence, iodide can be lost to the bed sediments or suspended sediments and this tracer will give inaccurate results for long tracer experiments.

Hence, on the Mures River System there is no practical alternative to using a mathematical approach to estimate dispersion coefficients. Essentially dispersion is changing all the time along a river as flows change, as slopes and geometry change and as velocity changes. Thus dispersion coefficients really need to be calculated at every time-step. As described above, the model uses the Fisher method to estimate dispersion coefficients (Chapra 1997). This approach is used

**Table 9** | Simulation results assuming scenario 3a under low-flow conditions with two decay coefficients

| Reach | Decay coeff 0.1 days$^{-1}$ Peak CN conc (mg l$^{-1}$) | Decay coeff 0.2 days$^{-1}$ Peak CN conc (mg l$^{-1}$) |
|---|---|---|
| Abrud | 4.67 | 4.65 |
| Campeni | 4.34 | 4.26 |
| Baia de Aries | 4.07 | 3.88 |
| Turda | 2.96 | 2.48 |
| Ocna Mures | 1.35 | 0.94 |
| Albalulia | 0.49 | 0.23 |
| Deva | 0.23 | 0.07 |
| Savirsin | 0.11 | 0.02 |
| Arad | 0.09 | 0.02 |
| Nadlac | 0.07 | 0.01 |

**Table 10** | Peak CN concentrations for scenario 3b for high-flow conditions

| Reach | Peak CN conc (mg l$^{-1}$) |
|---|---|
| Abrud | 0.87 |
| Campeni | 0.50 |
| Baia de Aries | 0.36 |
| Turda | 0.25 |
| Ocna Mures | 0.16 |
| Albalulia | 0.11 |
| Deva | 0.09 |
| Savirsin | 0.08 |
| Arad | 0.08 |
| Nadlac | 0.07 |

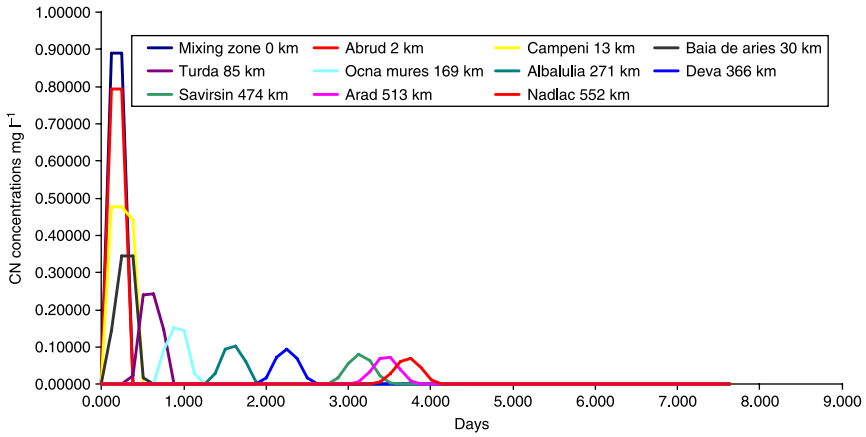


**Figure 10** | CN concentrations at a range of sites assuming scenario 3b with high-flow conditions.

to provide the best estimate of dispersion coefficient at all times, all velocities and all locations.

## SIMULATION RESULTS

The model has been applied to the river system assuming three sets of scenarios, these being a catastrophic event of the high precipitation Baia Mare type, dam burst events under a range of different conditions and finally dam bursts with increasingly larger volumes of water release over shorter time periods.

### Simulating the Baia Mare type event

Essentially with a Baia Mare type rainfall event the spillway on the Corna Valley Dam at Roşia Montană would come into operation and a 1 in 10 year flood spillway flow of $2.3\,m^3\,s^{-1}$ flow would occur with the set of concentrations shown in Table 4 or summer and winter conditions. It is assumed in the table and graphs below that the release of water via the spillway continues for a 12 hour period, a reasonable estimate of the response time and duration of the flow to a rainfall event. However, the model is set up so that any duration of release event can be simulated.

Tables 5 and 6 show the simulation results for a high rainfall event assuming the worse case condition of a release in year 17 when the concentration behind the dam is at its highest. Note the dam concentrations were calculated in a wide ranging environmental impact study (http://www.gabrielresources.com/i/pdf/EIA). These concentrations vary with time as the dam receives seasonal rainfall. Tables 5 and 6 show the low-flow conditions for events occurring in the summer and winter respectively. In both cases, the peak CN WAD concentrations at the border are low although the summer simulation is lower due to the loss of CN, due to volatilization and degradation, natural processes occurring in the river. The CN decay coefficient is set to $0.1\,d^{-1}$, a relatively low value. Essentially the long travel time of over 20 days in summer conditions provides sufficient time for the loss of CN along the river system. Table 7 shows the simulation in a winter high-flow condition. The peak concentrations are particularly low because of the large dilution effect of incoming streams and tributaries. The model results for the low-flow and high-flow simulations are shown in Figures 7 and 8.

**Table 11** | Simulated CN under scenario 3c for low-flow conditions

| Reach | Decay rate 0.1 days$^{-1}$ Peak CN conc (mg l$^{-1}$) | Decay rate 0.2 days$^{-1}$ Peak CN conc (mg l$^{-1}$) |
|---|---|---|
| Abrud | 4.37 | 4.37 |
| Campeni | 4.25 | 4.21 |
| Baia de Aries | 4.13 | 4.01 |
| Turda | 3.77 | 3.37 |
| Ocna Mures | 2.88 | 2.30 |
| Albalulia | 1.51 | 0.88 |
| Deva | 0.81 | 0.34 |
| Savirsin | 0.41 | 0.11 |
| Arad | 0.31 | 0.07 |
| Nadlac | 0.25 | 0.05 |

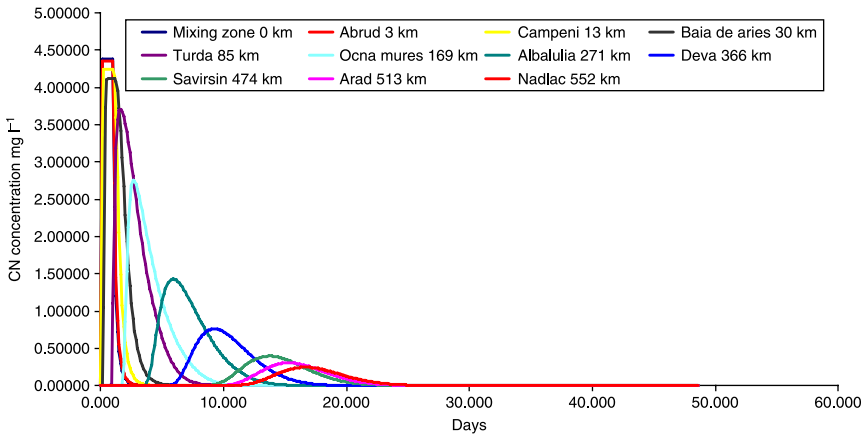


**Figure 11** | Low-flow scenario 3c with a decay rate of 0.1 day$^{-1}$.

It is clear from this analysis that a Baia Mare type rainfall and snow event will not produce the levels of pollution observed in the actual Baia Mare event (UNEP 2000). This is mainly because of the modern engineering design of a spillway that protects the dam from a dangerous build-up of water behind the dam wall.

## Dam burst scenarios

A dam break, releasing the water behind the dam over a short period of time, is a key event having a significant impact on the river system downstream. This has been investigated using the new dispersion model. As in the case of the previous INCA study, a range of flows and water quality conditions have been investigated. Table 8 gives a summary of the scenarios investigated in this study. These have focused on the low-flow conditions, but some high-flow runs have been undertaken to assess this type of incident. Two sets of dam break scenarios have been considered representing (1) start-up dam failure at the end of year 1 and (2) assuming final dam failure at year 17, when the dam is at its maximum size. The expected CN WAD concentrations released in each scenario are shown in Table 8 together with the maximum volumes of water released by the potential dam break. The scenarios considered in the study are again both low and high-flow conditions.

## Scenarios 3a and 3b

The simulations for scenario 3a (Table 8) are illustrated in Figure 9 and Table 9 for a range of decay coefficients under low-flow conditions. Under low-flow conditions the peak

**Table 12** | Simulated CN concentrations for scenario 3d under high-flow conditions with decay coefficient at 0.1 days$^{-1}$

| Reach | Peak CN conc (mg l$^{-1}$) |
|---|---|
| Abrud | 0.991 |
| Campeni | 0.574 |
| Baia de Aries | 0.416 |
| Turda | 0.295 |
| Ocna Mures | 0.184 |
| Albalulia | 0.127 |
| Deva | 0.116 |
| Savirsin | 0.105 |
| Arad | 0.100 |
| Nadlac | 0.096 |

**Table 13** | Simulated CN concentrations for scenario 3e under low-flow conditions

| Reach | Decay Rate 0.2 days$^{-1}$ Peak CN conc (mg l$^{-1}$) | Decay rate 0.1 days$^{-1}$ Peak CN conc (mg l$^{-1}$) |
|---|---|---|
| Abrud | 4.98 | 4.98 |
| Campeni | 4.88 | 4.84 |
| Baia de Aries | 4.77 | 4.65 |
| Turda | 4.44 | 4.04 |
| Ocna Mures | 3.76 | 3.12 |
| Albalulia | 2.33 | 1.48 |
| Deva | 1.37 | 0.65 |
| Savirsin | 0.73 | 0.23 |
| Arad | 0.57 | 0.15 |
| Nadlac | 0.46 | 0.11 |

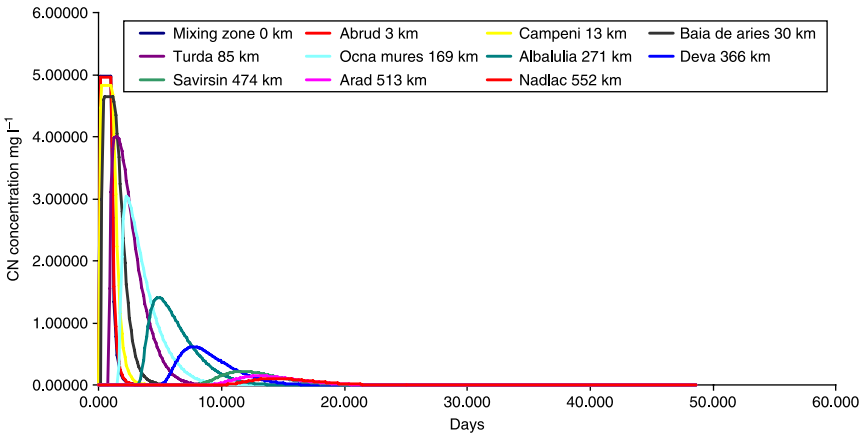


**Figure 12** | Scenario 3e with a decay of 0.2 day$^{-1}$ under low-flow conditions.

CN concentrations at the border will therefore be above the CN standard of 0.1 mg l$^{-1}$. Figure 9 shows the response along the river at key locations.

In the case of the 3b scenario (Table 8), we are assuming that the river is in a high-flow condition and hence dilution will be significant. This is illustrated in Table 10 and Figure 10.

## Scenario 3c and 3d

Scenarios 3c and 3d (Table 8) assume that the dam is in year 17 and has a water volume of 381,100 m$^3$ with a concentration of 4.4 mg l$^{-1}$ of CN WAD. The results of the peak concentrations for scenario 3c with two decay rates are shown in Table 11. Figure 11 illustrates the CN simulation at a range of locations along the river. The results suggest that given the higher discharge from the dam, the concentrations will exceed the limit with the lower decay rate. However, higher decay rates suggest lower concentrations at the border. Under high-flow conditions the model suggests that dilution will be significant and hence concentrations stay below the standard at the border, as shown in Table 12.

## Scenario 3e and 3f

Scenarios 3e and 3f (Table 8) assume that the dam is in year 17 and has a water volume of 5,880,800 m$^3$ with a concentration of 5.0 mg l$^{-1}$ of CN WAD. The results of the peak concentrations for the low-flow scenario 3e are shown in Table 13. Figure 12 illustrates the CN

**Table 14** | Simulated CN concentrations for scenario 3f under high-flow conditions

| Reach | Peak CN conc (mg l$^{-1}$) Decay coeff. 0.1 days$^{-1}$ | Peak CN conc (mg l$^{-1}$) Decay coeff. 0.2 days$^{-1}$ |
|---|---|---|
| Abrud | 1.43 | 1.43 |
| Campeni | 0.87 | 0.86 |
| Baia de Aries | 0.64 | 0.63 |
| Turda | 0.46 | 0.44 |
| Ocna Mures | 0.29 | 0.27 |
| Albalulia | 0.20 | 0.17 |
| Deva | 0.18 | 0.15 |
| Savirsin | 0.17 | 0.12 |
| Arad | 0.16 | 0.11 |
| Nadlac | 0.15 | 0.10 |

**Table 15** | Simulated CN concentrations for a range of spill durations from 24 hours to 1.5 hours for scenario 3a

| | Peak CN concentration (mg l$^{-1}$) | | | | |
|---|---|---|---|---|---|
| Spill duration (hr) | 24 | 12 | 6 | 3 | 1.5 |
| Abrud | 4.668 | 4.745 | 4.776 | 4.787 | 4.792 |
| Campeni | 4.341 | 4.546 | 4.656 | 4.711 | 4.736 |
| Baia de Aries | 4.069 | 4.343 | 4.474 | 4.523 | 4.521 |
| Turda | 2.963 | 3.047 | 3.060 | 3.068 | 3.023 |
| Ocna Mures | 1.347 | 1.368 | 1.375 | 1.383 | 1.390 |
| Albalulia | 0.492 | 0.500 | 0.504 | 0.507 | 0.510 |
| Deva | 0.234 | 0.238 | 0.240 | 0.242 | 0.243 |
| Savirsin | 0.114 | 0.116 | 0.117 | 0.118 | 0.118 |
| Arad | 0.087 | 0.089 | 0.090 | 0.090 | 0.090 |
| Nadlac | 0.070 | 0.071 | 0.072 | 0.072 | 0.072 |

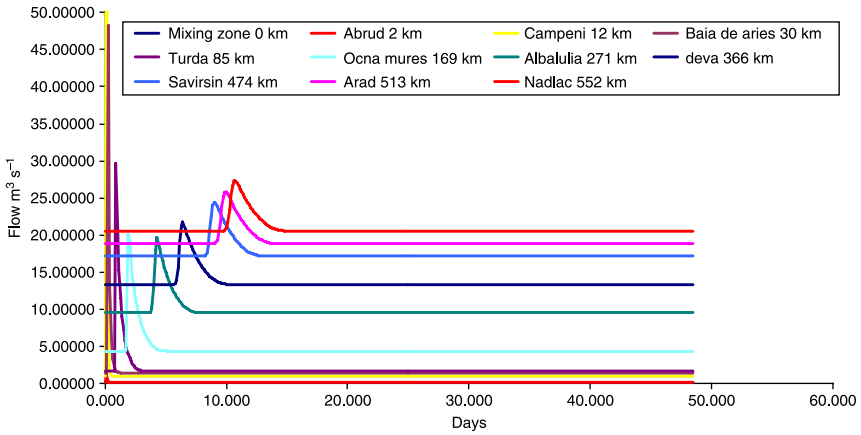


**Figure 13** | Flows simulated with a spill duration of 1.5 hrs.

simulation at a range of locations along the river. As might be expected with the high discharge rate under very low-flow conditions, the CN concentrations are higher at the border and exceed the standards. Table 14 shows the peak concentrations for scenario 3f assuming high flow conditions. As might be expected the concentrations are generally lower because of the increased dilution.

## Scenario runs assuming shorter discharge times

All the above scenarios assume that the discharge occurs over a 24 hour period. However, there could be a situation where the release times are shorter than this since the release time will depend on the nature of the dam break and the construction of the dam wall. The model has been used to assess the impacts in the event of a shorter release time. Table 15 shows the effect of reducing the duration of the spill from 24 hours to a range of durations, down to 1.5 hours. The results are initially counterintuitive, in that the reduced spill duration shows almost no differences at the lower reaches of the river. The reason for this is illustrated in Figures 13 and 14. In these figures are shown the simulated flow data for both the 24 hour and 1.5 hour spill duration. The figures indicate that although the flows are different in the top reaches of the river system due to the changed flows from the simulated dam break, by the time the flow gets some 100 km downstream, the flows in the two runs are almost identical. The velocities, dispersion and dilution effects will therefore be identical in both runs downstream. It is therefore not surprising that the concentrations are still very low 565 km downstream at the border.

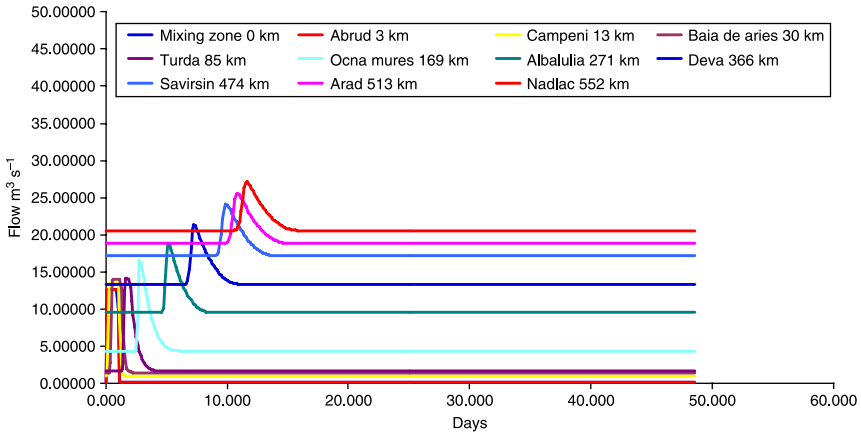


**Figure 14** | Flows simulated with a spill duration of 24 hours.

## CONCLUSIONS

The results presented here indicate the levels of pollution down the river system under a range of scenarios. These scenarios relate to low-flow and high-flow conditions and also to the duration of potential spills. In this paper, a new dispersion model is described in considerable detail together with the numerical solution techniques used to solve the equations. The model incorporates the dispersion and transport processes occurring in rivers and also accounts for the diluting effects of tributaries and runoff along the river. The model also allows for the degradation of pollutants along the river which, in the case of CN, is due to volatilization and chemical transformation to ammonia. This degradation depends on the residence time of the water in the river, temperature and the decay rate; the new model accounts for all these effects.

The model has been set up for the river system from the location of the proposed dam in the upstream catchment down to the border at Nadlac. The results indicate that in both high- and low-flow conditions, a Baia Mare type precipitation event will not produce a severe pollution impact. This is primarily because of the dam spillway which is designed to release water in a controlled manner during high rainfall conditions.

More problematic are the effects of a catastrophic dam break which would release all the water and pollutant content of the dam storage reservoir. The impact of the releases under different years of dam development is considered in this paper. The effect of the discharges under low-flow conditions is to generate low concentrations under most releases; all are below the CN standards except for the very largest volumes. This is because of the reduced dilution downstream in low-flow conditions as well as the significant dispersion and the large residence times. Dilution is also having a major effect in high-flow conditions creating relatively low concentrations, although the reduced travel time suggests that the year 17 dam releases will create higher pollution levels.

The question of the duration of the spill release has produced some very interesting results. Initially, the effects of reducing the spill duration say from 24 hours to 1.5 hours should be significant because the spill flow rates have to be much higher for the same mass of discharge. While this will have some effect in the upper reaches of the river, the impacts downstream at the border are negligible. This is because attenuation of the flood wave occurs and, after about 100 km of river, the pollution and flow pulse has mitigated so that it is indistinguishable from longer duration spills.

## ACKNOWLEDGEMENTS

The authors are extremely grateful to colleagues in Romania for the provision of data and for information for this research study. It should be emphasized that the opinions presented in the paper are solely those of the authors and the views expressed in the paper cannot be attributed to any other organization or group.

## REFERENCES

Aston, J. 2004 Aquatic environment management: a case study of the Rosia Montana gold mine project, Romania. In: Neal, C. & Littlewood, I. G. (eds), *Managing our aquatic environment in the 21st century: contemporary issues of water quality*. British Hydrological Society Occasional Paper No. 14, pp. 21–29. Available from http://www.hydrology.org.uk/publications/BHS_OP14d.pdf

Botz, M. & Mudder, T. 2001 Modeling of natural cyanide attenuation in tailings impoundments. *The Cyanide Compendium Mining*. Journal Books Ltd, London, UK.

Chapra, S. C. 1997 *Surface Water-Quality Modeling*. McGraw-Hill, New York.

Chapra, S. C. & Canale, R. P. 2006 *Numerical Methods for Engineers*. McGraw Hill, New York.

Fischer, H. B. 1968 Dispersion predictions in natural streams. *J. San. Eng. Div. ASCE* **94**(SA5), 927–944.

Fischer, H. B., List, E. I., Koh, R. C. Y., Imberger, J. & Brooks, N. H. 1979 *Mixing in Inland and Coastal Waters*. Academic, New York.

Johnson, D. B. & Hallberg, K. B. 2005 Acid mine drainage options: a review. *Sci. Total Environ.* **338**, 3–15.

Liu, H. 1977 Predicting dispersion coefficients in streams. *J. Environ. Eng. Div. ASCE* **103**(EE1), 59–69.

McQuivey, R. S. & Keefer, T. N. 1974 Simple method for predicting dispersion in streams. *J. Environ. Eng. Div. ASCE* **100**(EE4), 997–1011.

Mudder, T., Botz, M. & Smith, A. 2001 *Chemistry and Treatment of Cyanidation Wastes*, 2nd Edition. Mining Journal Books Ltd, London, UK.

Neal, C., Whitehead, P. G., Jeffery, H. & Neal, M. 2005 The Water Quality of the River Carnon, West Cornwall, November 1992

to March: the Impacts of Wheal Jane Discharges. *Sci. Total Environ.* **338**, 23–39.

Nordstrom, D. K., Alpers, C. N., Ptacek, C. J. & Blowes, D. W. 2000 Negative pH and extremely acidic mine waters from Iron Mountain, California. *Environ. Sci. Technol.* **34**, 254–258.

Rutherford, J. C. 1994 *River Mixing*. Wiley, New York.

Simovic, L., Snodgrass, W. J., Murphy, K. L. & Schmidt, J. W. 1984 Development of a model to describe the natural degradation of cyanide in gold mill effluents. *Proceedings of Conference on Cyanide and the Environment*, Tucson, Arizona, pp. 413–432.

UNEP 2000 *Cyanide Spill at Baia Mare Romania*. Report of the UNEP/OCHA Assessment Mission, Geneva.

Whitehead, P. G. & Prior, H. 2005 Bioremediation of Acid Mine Drainage: an Introduction to the Wheal Jane Wetlands Project. *Sci. Total Environ.* **338**, 15–21.

Whitehead, P. G., Williams, R. & Hornberger, G. E. 1986 On the identification of pollutant or tracer sources using dispersion theory. *J. Hydrol.* **84**, 273–286.

Whitehead, P. G., Hal!l, G., Neal, C. & Prior, H. 2005*a* Chemical Behaviour of the Wheal Jane Bioremediation System. *Sci. Total Environ.* **338**, 41–55.

Whitehead, P. G., Cosby, B. J. & Prior, H. 2005*b* The Wheal Jane Wetlands Model for Bioremediation of Acid Mine Drainage. *Sci. Total Environ.* **338**, 125–135.

Whitehead, P. G., Butterfield, D. & Wade, A. J. 2009 Simulating Metals and Mine Discharges in River Basins using a new Integrated Catchment Model for metals: Pollution impacts and Restoration strategies in the Aries-Mures river system in Transylvania, Romania. *Hydrol. Res.* **40**(2–3), 323–345.

First received 23 September 2008; accepted in revised form 5 January 2009